NANO LETTERS

LETTER

pubs.acs.org/NanoLett

Translocation of Single-Wall Carbon Nanotubes Through Solid-State Nanopores

Adam R. Hall,[*,†,‡] Johannes M. Keegstra,[†] Matthew C. Duch,[§] Mark C. Hersam,[§] and Cees Dekker[†]

[†]Kavli Institute of Nanoscience, Delft Technical University, 2628 CJ Delft, The Netherlands

[‡]Joint School of Nanoscience and Nanoengineering, University of North Carolina Greensboro, Greensboro, North Carolina 27401, United States

[§]Department of Materials Science and Engineering, Department of Chemistry, and Department of Medicine, Northwestern University, Evanston, Illinois 60208-3108, United States

ABSTRACT: We report the translocation of individual single-wall carbon nanotubes (SWNTs) through solid-state nanopores. Single-strand DNA oligomers are used to both disperse the SWNTs in aqueous solution and to provide them with a net charge, allowing them to be driven through the nanopores by an applied electric field. The resulting temporary interruptions in the measured nanopore conductance provide quantitative information on the diameter and length of the translocated nanotubes at a single-molecule level. Furthermore, we demonstrate that the technique can be utilized to monitor bundling of SWNT in solution by using complementary nucleotides to induce tube−tube agglomeration.

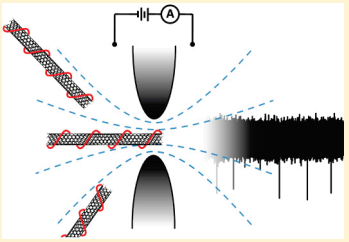

KEYWORDS: Solid-state nanopores, SWNT, nanotube, translocation, bundling

Solid-state nanopores[1] are a promising technique for the analysis of molecules on an individual basis. To date, nearly all studies with this system have focused on biomolecules like DNA,[2,3] RNA,[4] and proteins.[5,6] There is, however, a great deal of largely unexplored potential for their use in measuring nonbiological materials as well. One class of nanomaterial of particularly wide interest is the single-wall carbon nanotube (SWNT), a nanometer-scale diameter cylinder of graphene that has found utility in a variety of electrical and electromechanical devices including field-effect transistors,[7,8] transducers[9,10] and resonators.[11−13] While there have been several reports of techniques capable of handling bulk quantities of SWNT in aqueous solution,[14−16] evaluation of characteristics at the single tube level has thus far been relegated to surface techniques like scanning probe microscopies[17,18] and spectroscopic methods.[19,20] The application of the nanopore technique to this SWNT material would allow nanotubes to be interrogated at the individual level in solution. In this paper, we show that this is indeed feasible.

Two challenges exist in applying nanopore detection to nanotubes. First, SWNTs have no inherent charge and therefore experience no electrical driving force upon application of an electric field. Second, the hydrophobic nature of SWNTs prevents them from being readily dispersed in the aqueous solutions commonly used in nanopore analysis. In order to overcome both of these issues, the raw nanotube material is wrapped in short DNA oligomers. The use of DNA has two effects: the inherent charge of the DNA phosphate backbone imparts a net negative charge on the wrapped nanotubes, while its amphiphilic nature allows the SWNTs to be freely suspended in the aqueous measurement solution. The resultant material can therefore be introduced to one side of a nanopore in order to perform translocation measurements (Figure 1a).

Specifics of the nanopore device fabrication process have been described previously.[21] Briefly, standard microfabrication techniques are used in order to produce 20 nm thick, free-standing membranes of SiN supported by a larger silicon chip for handling. The highly focused beam of a transmission electron microscope is then used to locally ablate the membrane,[22] resulting in the formation of a single nanopore (Figure 1b, inset) with a sub-nanometer level of accuracy in diameter.[23] The nanopores used in the present work have diameters of 14−18 nm. The chip containing the single pore is loaded into a custom flow cell that allows solution to be introduced to both sides (cis- and trans-) of the membrane (Figure 1a). Electrical connection is made to each chamber by way of Ag/AgCl electrodes and current is recorded at 200 kHz using a patch-clamp amplifier (Axon 200B, Axon Instruments) and low-pass filtered at 100 kHz prior to digitization.

Preparation[24] of SWNT wrapped in $(AC)_{15}$ single-strand DNA oligomers begins by adding 2 mg mL^{-1} of SWNT soot (P2 nanotubes, Carbon Solutions, Inc.) to 70 mL of an aqueous solution of 1% (w/v) sodium cholate. The SWNTs are dispersed via treatment with horn ultrasonication (Fisher Scientific model 500 Sonic Dismembrator) for 1 h at a power of 55 W with an immersed tip. The average contour length of nanotubes after this treatment is 200 nm. The solution is centrifuged (SW 32 rotor, Beckman Coulter) at 32 krpm for 30 min to remove large aggregates, and the top 75% of the supernatant is retained. Next, a 0.1 M NaCl solution is prepared, containing $(AC)_{15}$ DNA oligomers (1.0 mg mL^{-1}) and the sodium cholate-wrapped SWNT material (~0.2 mg mL^{-1}). A three-day dialysis in a bath of 0.1 M NaCl is performed using a 3.5−5.0 kDa membrane (Spectrum

Received: March 16, 2011
Revised: April 19, 2011
Published: May 16, 2011

dx.doi.org/10.1021/nl200873w | *Nano Lett.* 2011, 11, 2446–2450

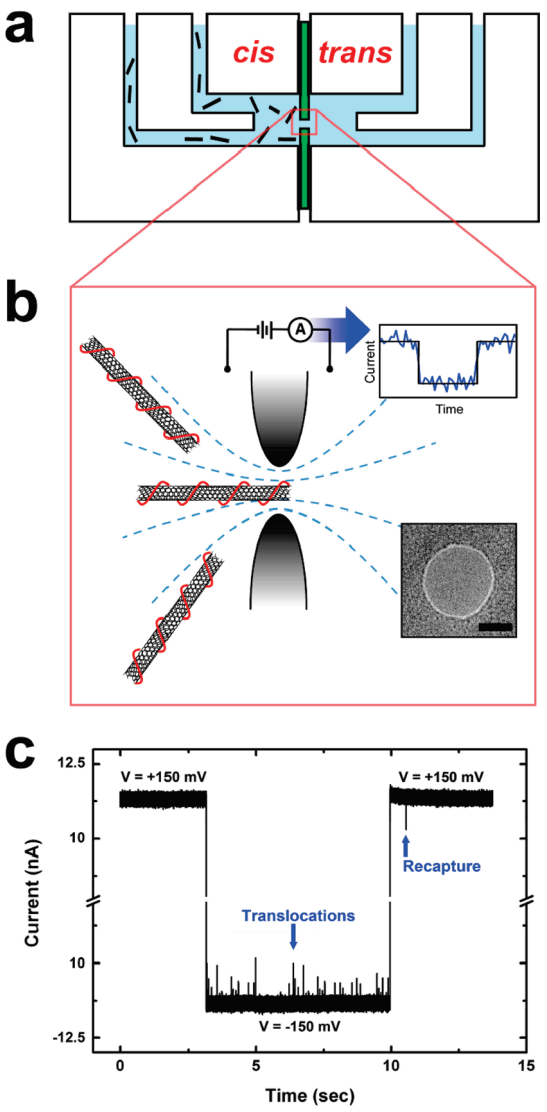

Figure 1. SWNT translocation through a solid-state nanopore. (a) Schematic of the translocation flow cell that surrounds an individual nanopore (green) and allows introduction of measurement solution to both sides. (b) Individual DNA-wrapped SWNT are driven electrically through a nanopore, resulting in temporary interruptions in the measured trans-pore current (top inset). Inset at bottom right: TEM image of a typical nanopore (scale bar 10 nm). (c) Current trace resulting from the application of voltage to the trans chamber of the flow cell. The current shows no spikes when +150 mV is applied (left), whereas a series of events is observed at −150 mV (middle), signaling carbon nanotube translocation. When +150 mV is again applied (right), return events are observed that vanish quickly, indicative of translocated molecules that are recaptured from the trans chamber back into the cis chamber.

Laboratories, Inc.) to slowly replace the sodium cholate with a ssDNA encapsulation layer. The solution is subsequently dialyzed for an additional seven days using a 100 kDa filter to remove excess oligomers and further purify the solution. The resultant material is added to a measurement solution containing 1 M KCl, 10 mM Tris-HCL (pH 8.0), and 1 mM EDTA. We estimate the final concentration of DNA-wrapped SWNTs to be about 30 μg mL^{-1}.

DNA-SWNT material is added to the cis chamber of the flow cell, and upon application of a voltage between the cis and trans chambers we observe characteristic spikes in the current measured through the nanopore (Figure 1c). In order to ensure that these are in fact translocation events and not merely stochastic interactions between material and the pore on the cis side only, we reverse the applied voltage, yielding "recapture" translocation events[25] for a limited time (Figure 1c, right). This demonstrates that the brief interruptions in the measured current indeed correspond to the passage of individual DNA-SWNTs through the pore. We observe that DNA-SWNT is found to move toward the negative electrode. This may be explained by considering the combination of electrophoresis and electroosmotic flow, which was demonstrated recently[26] to dictate translocation direction. Control experiments with clean measurement buffer and with measurement buffer containing only $(AC)_{15}$ oligomers at a concentration of 100 nM (data not shown) do not yield any events in either direction. Note that we do not expect to be able to detect oligomers alone, as their translocation times would be well below the measurement capabilities. Similar translocations of DNA-SWNTs were measured on more than 30 separate nanopores.

Having established that the translocation of DNA-wrapped SWNTs through solid-state nanopores can be measured, we now turn to a quantitative analysis of the characteristics of these events. Figure 2a shows a typical conductance trace. We observe a roughly uniform depth of events, indicating that the translocated molecules have a fairly narrow range of diameters. Indeed, a histogram of all measured conductance data points for 462 individual events confirms this (nanopore diameter 18 nm, Figure 2b), yielding a ΔG of 1.56 ± 0.48 nS, where the error denotes the standard deviation in the distribution. Measurements on two additional nanopores (also 18 nm diameter) with the same DNA-SWNT material (Figure 2c) yield ΔG of 1.52 ± 0.44 and 1.48 ± 0.59 nS, respectively, demonstrating the consistency and repeatability of the technique. A narrow distribution is expected if one assumes a roughly uniform ssDNA layer on the raw nanotubes that have diameters ranging from approximately 1.3 to 1.7 nm. The mean ΔG is found to be somewhat larger than that of dsDNA, the molecule most widely studied by nanopore translocations, which is measured as 1.1 nS under the same experimental conditions. Considering the 2.2 nm diameter of dsDNA and assuming the depth of the conductance blockades scales directly with cross-sectional area A of the translocating molecule, we can say

$$\frac{\Delta G_{\mathrm{SWNT}}}{\Delta G_{\mathrm{DNA}}} = \frac{A_{(\mathrm{AC})15+\mathrm{SWNT}}}{A_{\mathrm{DNA}}} = \frac{\pi}{4}\frac{(d_{\mathrm{SWNT}} + 2T_{\mathrm{AC}})^2}{\frac{\pi}{4}d_{\mathrm{DNA}}{}^2}$$

where d_{DNA} is dsDNA diameter, d_{SWNT} = 1.5 ± 0.2 nm is SWNT diameter, and T_{AC} is the thickness of the $(AC)_{15}$ layer wrapped around the SWNT, which is assumed to be conformal. Using the average conductance changes for each molecule, we can therefore estimate the thickness of the ssDNA layer on the nanotubes to be $T_{\mathrm{AC}} = 0.54 \pm 0.26$ nm. This is a very reasonable value for the likely structure with the nucleotide bases lying flush with the graphitic surface of the SWNT. We also note that only a single population of event depth is observed (Figure 2b, inset), which is in contrast with measurements on dsDNA,[2,3] which yield multiple levels corresponding to the passage of folded molecules. A single population is expected for SWNTs since they are relatively stiff with a persistence length (L_p) of ~800 nm,[27] (i.e., 16 times larger than dsDNA) and therefore are unable to fold during translocation.

dx.doi.org/10.1021/nl200873w |*Nano Lett.* 2011, 11, 2446–2450

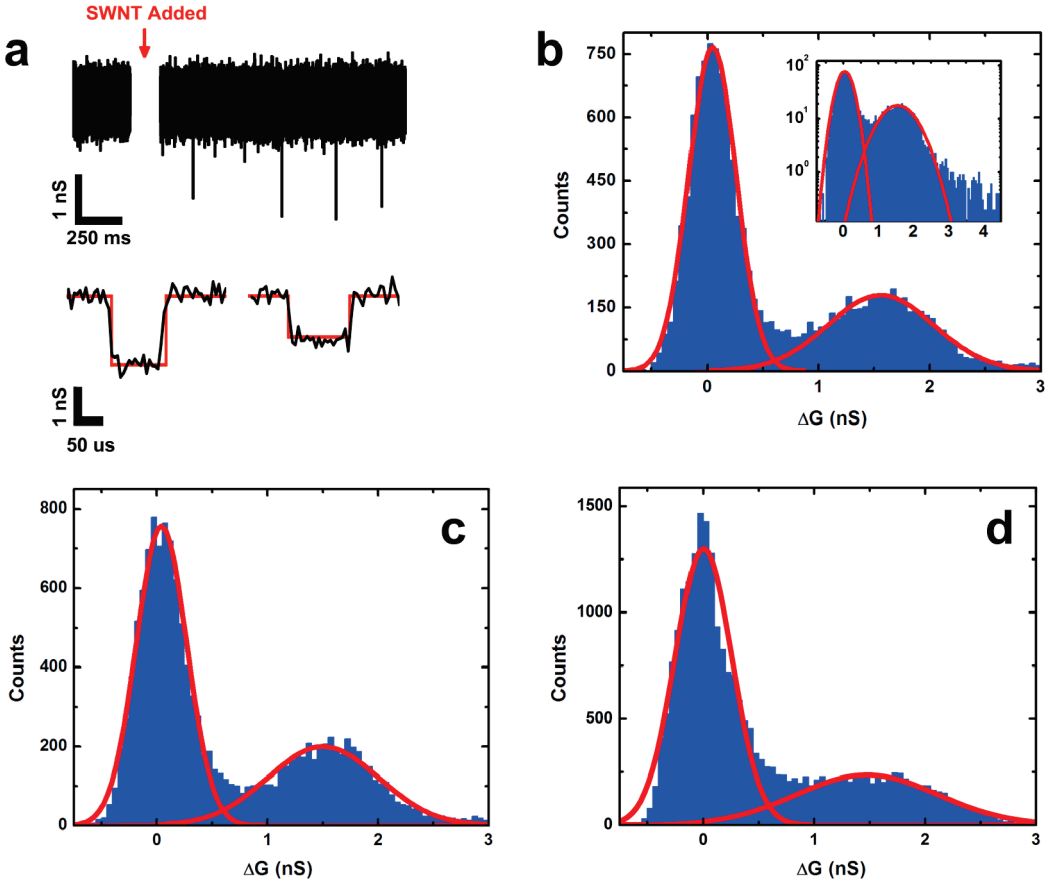

Figure 2. Analysis of SWNT translocations. (a) A typical conductance trace showing translocations upon the addition of SWNT material (top) and two typical blockages showing the pulselike event shape (bottom). Data are filtered at 100 kHz. (b) Histogram of conductance blockades through an 18 nm diameter pore (n = 462), yielding a population of points around 0 nS (the baseline conductance) and a population centered at 1.56 nS (SWNT). Inset: Log-scale plot of the same data, showing no additional populations at larger ΔG. (c,d) Translocation histograms (n = 467 (L) and 497 (R)) from two additional nanopores (diameters also 18 nm) demonstrating the reproducibility of the measurements.

The dwell time of the translocation events is shown in Figure 3a. We find a log-normal distribution (i.e., a Gaussian on a log scale) with a most probable dwell time Δt of 53 (+42, −24) μs, where the error denotes the half width at half-maximum (HWHM) of the distribution. This value is larger than the ∼7 μs dwell time anticipated for a similar length of dsDNA under similar solvent conditions based on the power law dependence measured previously,[28] reflecting the fact that the DNA-wrapped SWNTs have a lower linear charge density than dsDNA.[29] In total, the average speed of traversal for DNA-SWNT is 7.5 mm/s; about 7 times slower than the 55 mm/s value for 600 bp dsDNA as extrapolated from ref 29. Using our previously established parlance,[28] we note that this still qualifies as "fast" translocation, defined as the regime where $\Delta t \ll t_Z$, the upper bound on linear chain relaxation time (Zimm time). Since[30] $t_Z \sim R_g^3$ (where R_g is the radius of gyration) and in turn $R_g \sim L_p^{1/2}$, we estimate the SWNT t_Z to be 64 times larger than that of dsDNA, far outweighing the relatively small difference in dwell time. In the fast translocation regime, the rearrangement of the entropic coil has been implicated as the dominant source that sets the threading speed of dsDNA.[28] The high stiffness of SWNTs[27] prevents them from forming this entropic coil, suggesting a more immediate link between dwell time and molecular length. It is this difference that makes a direct comparison between dsDNA translocation time and SWNT translocation time problematic. Interestingly, the observed log-normal distribution of Δt closely matches the shape of SWNT contour length distribution of 0.15 (+0.20, −0.09) μm as independently measured by AFM[31] (Figure 3b). This supports our assertion and indicates that nanopore translocation holds potential for fast characterization of SWNT lengths.

One important nanotube characteristic that is easily accessible by the present nanopore technique is nanotube bundling. SWNTs are often integrated into fabrication processes via deposition from solvent-based suspensions. Current production techniques[32,33] can currently create large amounts of pristine raw nanotube material, but van der Waals interactions between nanotubes lead to the formation of aggregates known as bundles. These nanotube bundles complicate the characterization and utilization of SWNTs in applications and can even mask their outstanding electronic and optical properties.[34] Proper dispersion is thus a key factor. However, techniques to accurately characterize the bundling over time are relatively scarce.[35,36] Consequently, we now show that bundling among DNA-SWNTs in solution can be assessed quickly with nanopores.

Two sets of nanotube material were prepared: one as described above and a second prepared in the same way except using DNA oligomers with an $(AT)_{15}$ sequence instead. In this way, the ability of adenine to hybridize with thymine can be exploited to induce bundling by causing interactions between the

dx.doi.org/10.1021/nl200873w |Nano Lett. 2011, 11, 2446–2450

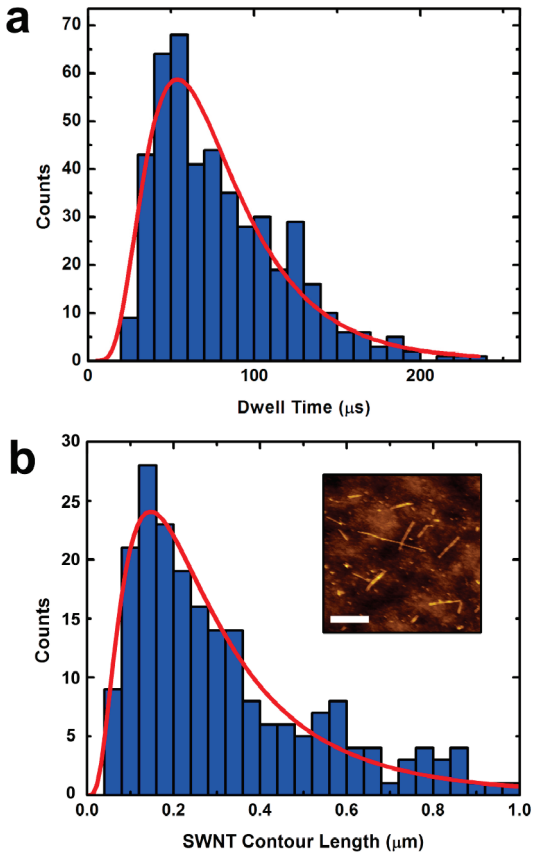

Figure 3. Dwell time and length distributions. (a) Dwell time statistics for the SWNT translocation data of Figure 2b, yielding a log-normal distribution centered at 53 μs. (b) Distribution of SWNT contour lengths as measured by AFM,[31] which is also observed to fit a log-normal distribution. Inset shows an example AFM image of the nanotube material (scale bar 500 nm).

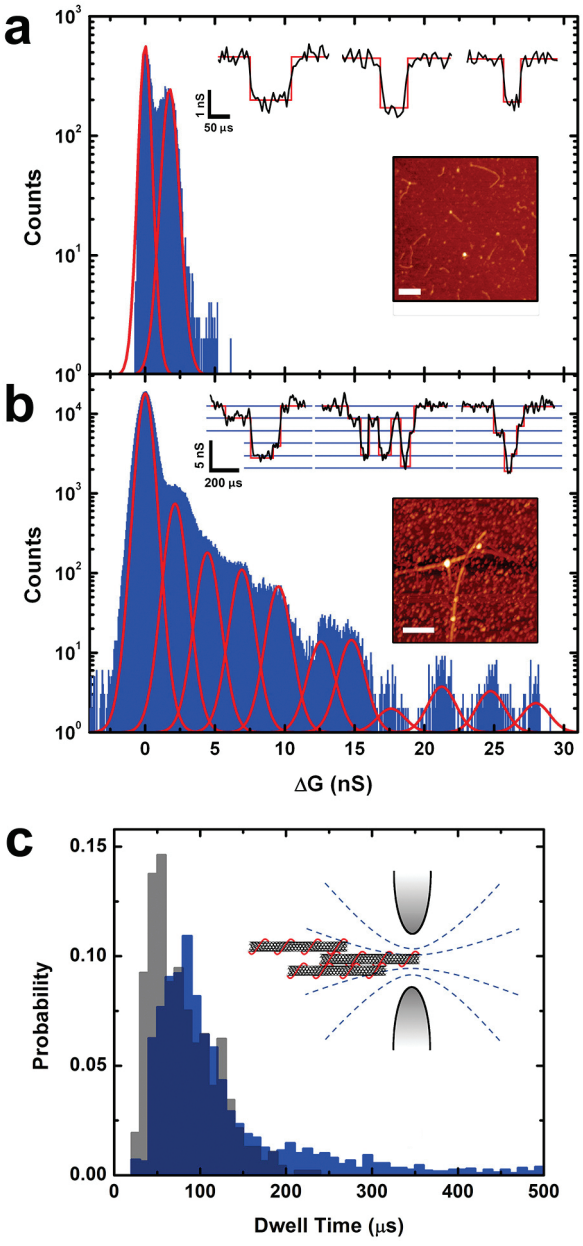

Figure 4. SWNT bundling in solution. (a) Histogram of all conductance data points for translocations measured on $(AC)_{15}$-SWNT material. Top insets show typical translocation events. Bottom inset shows an AFM image of the well-separated $(AC)_{15}$-SWNTs with typical height of 1−1.5 nm (z color scale 2 nm, scale bar 100 nm). (b) Histogram of all conductance data points for translocation events (n = 2463) measured on $(AT)_{15}$-SWNT material. Both data sets were recorded on nanopores with diameters of 14 nm. Top insets show typical individual translocation events (note the different vertical scale as compared to panel a example events). Bottom inset shows an AFM image of a typical agglomerate of $(AT)_{15}$-SWNTs with typical height of 4−5 nm (z color scale 10 nm, scale bar 300 nm). (c) Dwell time histograms for $(AC)_{15}$-SWNT (gray) and $(AT)_{15}$-SWNT (blue). Inset depicts unevenly bundled tubes responsible for the longer dwell times measured for $(AT)_{15}$-SWNT.

nucleotides surrounding one SWNT with those surrounding another. First, $(AC)_{15}$-SWNTs are translocated through a nanopore with diameter 14 nm. The resultant histogram of all measured conductance data points for 461 events (Figure 4a) yields a single population of ΔG outside of the baseline conductance, similar to those shown above. Subsequently, $(AT)_{15}$-SWNTs are translocated through a nanopore with the same diameter.[37] A strikingly different distribution is measured. Up to 10 populations can be discerned in the conductance histogram (Figure 4b), while individual event traces reveal a complex structure (insets to Figure 4b). As SWNTs are too stiff to fold on themselves through the narrow constriction of a nanopore, these observations indicate the translocation of SWNT bundles where multiple tubes are bound to each other through AT-TA bonding. Comparing the dwell time histograms of $(AC)_{15}$- and $(AT)_{15}$-SWNTs (Figure 4c), we find a higher average Δt for the latter with a much longer tail. The very long $(AT)_{15}$-SWNT dwell times, measuring more than an order of magnitude longer than for $(AC)_{15}$-SWNTs, can be attributed to long chains of individual SWNTs that are linked to each other by AT-TA bonding. These measurements thus demonstrate the ability to use nanopore translocations to elucidate bundling of DNA-wrapped SWNTs in solution.

We have presented here the first evidence of translocation of SWNTs through a solid-state nanopore. We used DNA oligomers of sequence $(AC)_{15}$ to wrap the SWNTs, thereby making them soluble in ionic solution and giving them a net charge. When added to one side of a nanopore, an applied electric field can be used to drive the DNA-wrapped SWNTs through the

dx.doi.org/10.1021/nl200873w |*Nano Lett.* 2011, 11, 2446–2450

opening, resulting in a series of well-defined interruptions in the measured trans-pore conductance. Analysis of DNA-SWNT translocation events revealed an average ΔG of 1.56 ± 0.48 nS, which is in agreement with expectations based on diameter. The dwell time distribution yielded an average Δt of 53 (+42, −24) μs. These times are significantly slower than dsDNA of the same size due to reduced charge density along the passing molecule. To further demonstrate the utility of nanopore measurements on SWNTs, we showed direct characterization of SWNT bundling in solution. While realized here for SWNTs, this approach can likely be expanded to other nanomaterials, thus presenting new opportunities for efficient nanoscale characterization at the single-molecule level.

AUTHOR INFORMATION

Corresponding Author
*E-mail: adam.hall@uncg.edu.

ACKNOWLEDGMENT

This work was supported by the European Union's Seventh Framework Programme (FP7/2007-2013) under Grant Agreement 201418 (READNA), ERC-2009-AdG Grant 247072 NANOFORBIO, the National Science Foundation (DMR-1006391), and National Institutes of Health (Training Grant T32HL076139).

REFERENCES

(1) Dekker, C. *Nat. Nanotechnol.* **2007**, *2* (4), 209–215.
(2) Li, J. L.; Gershow, M.; Stein, D.; Brandin, E.; Golovchenko, J. A. *Nat. Mater.* **2003**, *2* (9), 611–615.
(3) Storm, A. J.; Chen, J. H.; Zandbergen, H. W.; Dekker, C. *Phys. Rev. E: Stat., Nonlinear, Soft Matter Phys.* **2005**, *71* (5 Pt 1), 051903.
(4) Skinner, G. M.; van den Hout, M.; Broekmans, O.; Dekker, C.; Dekker, N. H. *Nano Lett.* **2009**, *9* (8), 2953–2960.
(5) Fologea, D.; Ledden, B.; McNabb, D. S.; Li, J. L. *Appl. Phys. Lett.* **2007**, *91* (5), 053901.
(6) Talaga, D. S.; Li, J. L. *J. Am. Chem. Soc.* **2009**, *131* (26), 9287–9297.
(7) Tans, S. J.; Verschueren, A. R. M.; Dekker, C. *Nature* **1998**, *393* (6680), 49–52.
(8) Javey, A.; Guo, J.; Wang, Q.; Lundstrom, M.; Dai, H. J. *Nature* **2003**, *424* (6949), 654–657.
(9) Minot, E. D.; Yaish, Y.; Sazonova, V.; Park, J. Y.; Brink, M.; McEuen, P. L. *Phys. Rev. Lett.* **2003**, *90* (15), 156401.
(10) Hall, A. R.; Falvo, M. R.; Superfine, R.; Washburn, S. *Nat. Nanotechnol.* **2007**, *2* (7), 413–416.
(11) Sazonova, V.; Yaish, Y.; Ustunel, H.; Roundy, D.; Arias, T. A.; McEuen, P. L. *Nature* **2004**, *431* (7006), 284–287.
(12) Witkamp, B.; Poot, M.; van der Zant, H. S. J. *Nano Lett.* **2006**, *6* (12), 2904–2908.
(13) Hall, A. R.; Falvo, M. R.; Superfine, R.; Washburn, S. *Nano Lett.* **2008**, *8* (11), 3746–3749.
(14) Arnold, M. S.; Green, A. A.; Hulvat, J. F.; Stupp, S. I.; Hersam, M. C. *Nat. Nanotechnol.* **2006**, *1* (1), 60–65.
(15) Huang, X. Y.; McLean, R. S.; Zheng, M. *Anal. Chem.* **2005**, *77* (19), 6225–6228.
(16) Krupke, R.; Hennrich, F.; von Lohneysen, H.; Kappes, M. M. *Science* **2003**, *301* (5631), 344–347.
(17) Heo, J. S.; Bockrath, M. *Nano Lett.* **2005**, *5* (5), 853–857.
(18) Venema, L. C.; Meunier, V.; Lambin, P.; Dekker, C. *Phys. Rev. B* **2000**, *61* (4), 2991–2996.
(19) Hartschuh, A.; Sanchez, E. J.; Xie, X. S.; Novotny, L. *Phys. Rev. Lett.* **2003**, *90* (9), 095503.
(20) Joh, D. Y.; Herman, L. H.; Ju, S.; Kinder, J.; Segal, M.; Johnson, J. N.; Chan, G. K. L.; Park, J. *Nano Lett.* **2011**, *11* (1), 7.
(21) Krapf, D.; Wu, M. Y.; Smeets, R. M. M.; Zandbergen, H. W.; Dekker, C.; Lemay, S. G. *Nano Lett.* **2006**, *6* (1), 105–109.
(22) Storm, A. J.; Chen, J. H.; Ling, X. S.; Zandbergen, H. W.; Dekker, C. *J. Appl. Phys.* **2005**, *98* (1), 014307.
(23) Storm, A. J.; Chen, J. H.; Ling, X. S.; Zandbergen, H. W.; Dekker, C. *Nat. Mater.* **2003**, *2* (8), 537–540.
(24) Barone, P. W.; Baik, S.; Heller, D. A.; Strano, M. S. *Nat. Mater.* **2005**, *4* (1), 86.
(25) Gershow, M.; Golovchenko, J. A. *Nat. Nanotechnol.* **2007**, *2* (12), 775–779.
(26) Firnkes, M.; Pedone, D.; Knezevic, J.; Doblinger, M.; Rant, U. *Nano Lett.* **2010**, *10* (6), 2162–2167.
(27) Sano, M.; Kamino, A.; Okamura, J.; Shinkai, S. *Science* **2001**, *293* (5533), 1299–1301.
(28) Storm, A. J.; Storm, C.; Chen, J. H.; Zandbergen, H.; Joanny, J. F.; Dekker, C. *Nano Lett.* **2005**, *5* (7), 1193–1197.
(29) Zheng, M.; Jagota, A.; Strano, M. S.; Santos, A. P.; Barone, P.; Chou, S. G.; Diner, B. A.; Dresselhaus, M. S.; McLean, R. S.; Onoa, G. B.; Samsonidze, G. G.; Semke, E. D.; Usrey, M.; Walls, D. J. *Science* **2003**, *302* (5650), 1545–1548.
(30) Rubinstein, M.; Colby, R. H. *Polymer Physics*, 1st ed.; Oxford University Press: New York, 2003.
(31) Green, A. A.; Hersam, M. C. *Nat. Nanotechnol.* **2009**, *4* (1), 64–70.
(32) Thess, A.; Lee, R.; Nikolaev, P.; Dai, H. J.; Petit, P.; Robert, J.; Xu, C. H.; Lee, Y. H.; Kim, S. G.; Rinzler, A. G.; Colbert, D. T.; Scuseria, G. E.; Tomanek, D.; Fischer, J. E.; Smalley, R. E. *Science* **1996**, *273* (5274), 483–487.
(33) Journet, C.; Maser, W. K.; Bernier, P.; Loiseau, A.; delaChapelle, M. L.; Lefrant, S.; Deniard, P.; Lee, R.; Fischer, J. E. *Nature* **1997**, *388* (6644), 756–758.
(34) O'Connell, M. J.; Bachilo, S. M.; Huffman, C. B.; Moore, V. C.; Strano, M. S.; Haroz, E. H.; Rialon, K. L.; Boul, P. J.; Noon, W. H.; Kittrell, C.; Ma, J. P.; Hauge, R. H.; Weisman, R. B.; Smalley, R. E. *Science* **2002**, *297* (5581), 593–596.
(35) Eda, G.; Fanchini, G.; Kanwal, A.; Chhowalla, M. *J. Appl. Phys.* **2008**, *103*, 093118.
(36) Marquis, R.; Greco, C.; Schultz, P.; Meunier, S.; Mioskowski, C. *J. Nanosci. Nanotechnol.* **2009**, *9* (11), 6777–6782.
(37) For $(AT)_{15}$-SWNT translocations, measurement solution included 0.01% (v/v) POP-6 rather than Tween-20. This surfactant alone was found to cause some conductance instabilities at very low values, <1 nS (lower than the first SWNT peak). We note that the broader $(AT)_{15}$-SWNT bundles are observed to move towards the positive electrode, further highlighting the intricate relationship of electrophoresis and electroosmosis in the translocation process.